Secondary aerosol formation from dimethyl sulfide

SMOG CHAMBER EXPERIMENTS AND DETAILED PROCESS MODELLING

Author
Dana LÜDEMANN

Supervised by
Pontus ROLDIN

THESIS SUBMITTED FOR THE DEGREE OF BACHELOR OF SCIENCE
PROJECT DURATION: 4 MONTHS (HALFTIME)

LUND UNIVERSITY

Department of Physics | Division of Nuclear Physics| May 2020

Abstract

The aim of this thesis was to investigate the secondary aerosol formation from dimethyl sulfide (DMS) using the aerosol dynamics, gas- and particle-phase chemistry kinetic multi-layer model, ADCHAM. The first simulations, concerning the butanol oxidation via hydroxyl radicals (OH), were performed to characterize the UV-light source of the AURA smog chamber (Aarhus university, Denmark), later used for the DMS experiments. The observed, strong impact of the relative humidity (RH) on the OH-concentration during the butanol-OH experiments may be related to the chamber walls, however, the modelled OH concentrations were not sensitive to the RH or the absolute water molecule concentration. The DMS oxidation via OH and subsequent secondary aerosol formation was simulated and compared to the measurements from the smog chamber experiments conducted at AURA. The results show that the recently observed DMS oxidation product hydroperoxymethyl thioformate (HPMTF) has most likely a negligible contribution to the new particle formation and further, the secondary particle formation from methanesulfonic acid (MSA) condensation is highly sensitive to the ammonia (NH_3) concentration and RH in the chamber. The final atmospheric DMS tests investigated the impact of the multi-phase (gas, particle, cloud) DMS chemistry involving halogens (Cl, Br, I) emitted from the ocean surface. Adding representative ocean halogen emissions as well as idealised aqueous-phase cloud passages led to increasing MSA and sulfuric acid (H_2SO_4) aerosol particle mass, but not increasing particle number concentrations. This could indicate that neglecting these processes may lead to inaccurate predictions of the indirect radiative climate effect of DMS-aerosols.

Contents

Abbreviations

ACDC	Atmospheric Cluster Dynamics Code
ADCHAM	Aerosol Dynamics, Gas- and Particle-phase Chemistry Kinetic Multi-layer Model
CCN	Cloud Condensation Nuclei
DMS	Dimethyl Sulfide
HPMTF	Hydroperoxymethyl Thioformate
IPCC	Intergovernmental Panel on Climate Change
MSA	Methanesulfonic Acid
MSIA	Methanesulfinic Acid
PM	Particulate Matter
RF	Radiative Forcing
RH	Relative Humidity
SOA	Secondary Organic Aerosol
VOC	Volatile Organic Compound

1 Introduction

The suspension of solid or liquid particles in a mixture of gases is known as an aerosol and can be found everywhere on Earth. Starting from about one nanometer to several micrometers, the size of these particles is as diverse as their origin. Particles emitted directly into the atmosphere (e.g. windblown dust) make up primary aerosol particles, whereas the condensation and nucleation of gases forms secondary aerosol particles [1].

Despite the small particle size and variety of chemical compositions, aerosols in the atmosphere have a significant influence on Earth's Climate. In general, aerosols affect Earth's climate directly by scattering incoming solar radiation or indirectly by serving as nuclei for cloud droplet formation [1].

In 1987, the atmospheric scientist Robert J. Charlson published an article identifying the dimethyl sulfide (DMS) emission of bacteria on the ocean surface as main source for cloud condensation nuclei (CCN) and major source of sulfur over the oceans [2]. Hence, DMS may have a large impact on marine cloud properties, as well as the global climate. Most reaction pathways of the DMS chemistry have been extensively studied (Hoffmann et al.[3], Barnes et al.[4], Bräuer et al.[5]), however there is lack of detailed knowledge about the aqueous-phase DMS reactions (e.g. dissolution in clouds), halogen-DMS reactions and fate of the DMS oxidation products in the atmosphere. All these processes affect the secondary aerosol formation and the estimations of the total climate impact of DMS-aerosols.

During two measuring campaigns conducted at the AURA smog chamber in Aarhus, the DMS oxidation via hydroxyl radicals (OH) was investigated. This thesis focuses on simulating some of these experiments using the aerosol dynamics, gas- and particle-phase chemistry kinetic multi-layer model, ADCHAM [6]. Moreover, this thesis seeks to give insight into how the DMS oxidation products such as sulfuric acid (H_2SO_4), methane sulphinic acid (MSIA), methanesulfonic acid (MSA) and the recently observed hydroperoxymethyl thioformate (HPMTF) [7] contribute to the aerosol particle formation, and further, how the particle formation is affected by different environmental conditions (e.g. UV-light intensity, relative humidity (RH), initial concentrations of trace gases).

During additional atmospheric relevant simulations with ADCHAM, the influence of idealized cloud passages and DMS gas- and aqueous-phase chemistry involving halogen species is investigated. Here, the main research questions concern the effect of halogen emission and aqueous-phase reactions on the particle formation, as well as looking into potential atmospheric climate implications from DMS-aerosols.

2 Background

Aerosol particles are categorized into primary and secondary particles depending on their emission into the atmosphere. However, they can be further divided according to their origin. Atmospheric aerosols can stem from natural sources or anthropogenic (human made) sources [1]. A major anthropogenic source is the emission from combustion of fossil fuels, i.e. coal and oil.

As mentioned in the introduction, primary aerosol particles (coarse particles) are directly emitted from a source such as windblown dust, volcanic eruptions or sea spray. In contrast, secondary aerosol particles are generated by a gas-to-particle phase conversion, i.e. condensation of certain gas species known as aerosol precursors. The main topic of this thesis is the formation and growth of these secondary aerosol particles which is dictated by three important processes: nucleation, condensation and coagulation (see figure 1).

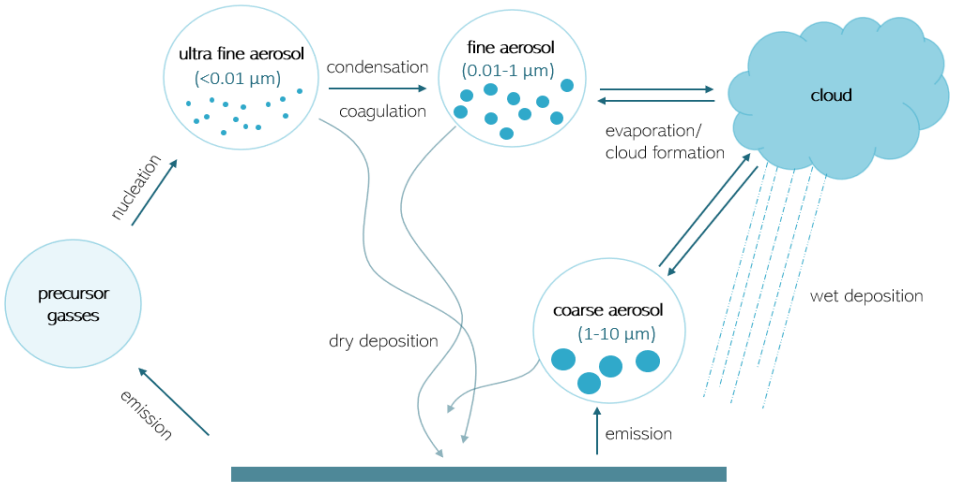

Figure 1: The schematic of an aerosol formation and removal process in the atmosphere including the relevant particle size ranges. The emission via precursor gases forms secondary aerosols, whilst the direct emission as coarse particles makes up a primary/coarse aerosols. The wet deposition removes both the particles that activate and form cloud droplets (in cloud scavenging) and the particles in all size ranges below the clouds (below cloud scavenging). (Reproduced from Fig. 8-2 in: *Introduction into Atmospheric Chemistry* [1])

2.1 Aerosol formation

Atmospheric aerosols are created by complex chemical and physical processes. In order to be defined as an aerosol particle, the particle has to be stable in the suspended gas for at least a few seconds. A vapour, different to an aerosol particle, is a substance in gas-phase which can undergo a phase transition (via nucleation or condensation, see below) into a liquid or solid phase, by for example increasing the vapour pressure (concentration) while keeping the temperature fixed.

The vapour pressure limit at which the gas-to-liquid or gas-to-solid phase-transition is possible is called the saturation vapour pressure. The saturation vapour pressure further depends on the existing liquid and solid phases (e.g. existence of aerosol particles). In general, when the saturation vapour pressure is reached above a certain surface (liquid or solid), the condensable vapour (e.g. water) is in an equilibrium state at which there is no net loss or uptake of the substance from or towards the surface, and thus, no net gas-surface mass transfer. A net loss from a solid or liquid phase to the gas-phase is called evaporation, while a net uptake from the gas-phase towards the solid or liquid phase is known as condensation.

The partial pressure of a vapour (or gas) in a mixture of gases is defined as the pressure the vapour would exert if it was to occupy the entire volume of the mixture by itself [8]. From this, the saturation ratio S_R can be derived which is the ratio of the partial pressure of a vapor to the saturation vapour pressure at a certain temperature. Once the S_R is larger than 1, the vapour is supersaturated; when the S_R equals 1, the vapour is saturated; and when the S_R is smaller than 1 the vapour is unsaturated [8].For water, this saturation ratio in percentage is often known as the relative humidity (RH).

Organic compounds are continuously released into the atmosphere from biogenic (produced by living organisms) and anthropogenic sources. On a global scale, roughly 1000 Tg of volatile organic compounds (VOC's) are emitted naturally each year [9]. Volatile organic compounds have a high vapour pressure meaning their molecules evaporate easily, and are therefore emitted as gases from certain solids or liquids. Most importantly, the oxidation of VOC's forms secondary organic aerosols (SOA), which make up about 50-85% of the total organic aerosols on Earth [9].

Starting from the emission of a VOC into the atmosphere, the VOC oxidizes (gets more low-volatile) in one or several steps into a non-condensable aerosol precursor gas. An example for a precursor gas is sulfur dioxide (SO_2) which forms sulfuric acid (H_2SO_4) via oxidation in the atmosphere [1]. As most atmospheric relevant condensable vapours, sulfuric acid has a relatively low vapour pressure w.r.t. most aerosol particle surfaces and will undergo a phase transfer from gas to liquid particulate matter (condensation).

A key-process of aerosol formation is nucleation, which can be either homogeneous or heterogeneous. Homogeneous nucleation is defined as new particle formation from a supersaturated vapour without the presence of condensation nuclei or ions [8]. The nucleation process is set off by a vapor, such as an aerosol precursor gas, which is easily supersaturated under atmospheric pressure. The vapour molecules attract each other due to for example van der Waals forces and assemble to clusters. Although, the clusters are continuously formed, they are unstable and will fall apart until a certain diameter d (Kelvin diameter) is reached. Exceeding the Kelvin diameter makes a cluster thermodynamically stable such that the resulting particle will grow by condensation.

The equation (1) shows the Kelvin ratio (K_R), which defines the saturation ratio required for an equilibrium between cluster growth and disintegration. A cluster of a given substance has the vapour pressure p_d at the curved surface and p_s at a plane surface.

$$K_R = \frac{p_d}{p_s} = \exp\left(\frac{4\gamma M}{\rho R T d^*}\right), \tag{1}$$

where γ, M, ρ and d^* denote the droplet surface tension, molar mass, density and diameter, and, R and T are the gas constant and the absolute temperature, respectively. From this equation (1) the Kelvin diameter can be derived [8]. However, the Kelvin ratio only applies to pure substances such that this can be seen as a model and simplification of the reality.

A reason for the supersaturation requirement of the vapor is that it increases the number concentration of the clusters, meaning, clusters are formed in all vapors, but the probability of reaching the stable kelvin diameter is lowered without supersaturation. In general, homogeneous nucleation leads to the formation of ultra-fine aerosols with a particle size of 1-2 nm [1].

Heterogeneous nucleation, also known as nucleated condensation, is the particle formation and growth in the presence of condensation nuclei or ions. This form of nucleation is the main process for cloud formation in the atmosphere [8].

The most important process for particle growth in the atmosphere is condensation. During this process mass is transferred from the gas-phase to the particulate-phase leading to particle growth. In the contrary, evaporation is the opposite process where mass is transferred from particulate- to the gas-phase. The process of condensation also requires a vapour that is supersaturated.

When aerosol particles collide with another and adhere to form larger particles, it is known as coagulation. During this process larger particles are formed, resulting in a continuous decrease in the number concentration of particles in the aerosol, but no change in the particle mass [8]. Coagulation can take place as thermal coagulation or kinematic coagulation. Thermal coagulation is a spontaneous and recurrent event in aerosols, and is caused by a Brownian relative motion between the particles. On the other hand, kinematic coagulation is driven by external forces (e.g. gravity or electromagnetic forces) that dictate the inter-particle relative motion [8].

The growth from both Brownian coagulation and condensation leads to fine aerosols with a particle size of 0.01-1 µm (Fig. 1). After 1 µm the growth slows down due to the size of the particles prohibiting rapid condensation and decreasing the relative motion (i.e. the coagulation rate) [1]. The above described aerosol dynamics processes (nucleation, condensation and coagulation) typically result in the formation of distinct and approximately log normal distributed particle modes (Fig. 2).

Typically, particles larger than $\sim$100 nm in diameter have the potential to be active as cloud condensation nuclei (form cloud droplets) at atmospheric relevant conditions. While small particles can be removed from the atmosphere by coagulation, larger particles can be removed by wet and dry depositions (e.g. rainout or gravitational sedimentation) [10].

2.2 Particle distributions and concentrations

The parametrisation of an aerosol's nature and behaviour is best described by the particle size since all properties depend on it. For simplicity, the shape of all aerosol particles is assumed to be spherical. The particle size can range from 0.001- to 100 µm and refers to the diameter of the particle.

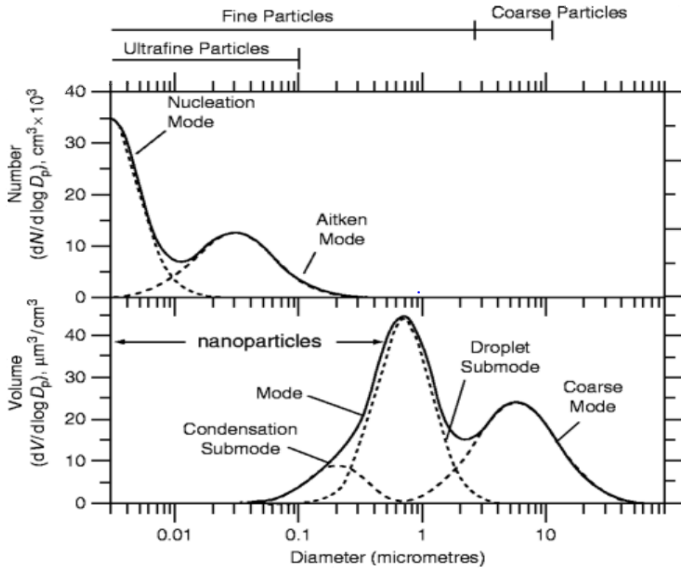

Figure 2: Typical log normal particle number and volume size distributions of an atmospheric aerosol including different modes. (Reprint/Reuse by permission from Spinger Nature: Springer Nature, Adhesion of Nanoparticles by Kevin Kendall, Michaela Kendall, Florian Rehfeldt, Jan 1, 2010.)

Most aerosols are poly-dispersed meaning they consist of a vast variety of particle sizes forming a number size distribution that needs to be evaluated statistically. The number size distribution gives the fraction of the total number concentration of particles in any size range [8]. The same holds for the mass, volume and surface size distribution as function of particle size. There are several mathematical approximations to describe an aerosol distribution which can overall be categorized into discrete or analytical approximations. Since the range of particle size is so large, atmospheric aerosols are often described by normal distributions under a logarithmic scale (log-normal distribution).

The figure 2 shows an example of a number and volume size distribution. The number size distribution is mostly dominated by secondary aerosol particles, while mass or volume size distributions are often dominated by primary aerosol particles. Particle size distributions typically display one or several modes (see figure 2) which result from different aerosol formation and removal processes. The modes overlap in size spectrum due to a continuous change of particles sizes from condensation, coagulation and evaporation.

The mass concentration of aerosol particles is the most measured property, especially concerning population health and environmental effects. The mass concentration indicates the mass of particulate matter (PM) in a unit volume of air [8]. For instance, the mass con-

centration of atmospheric aerosol particles above open oceans typical amounts to about 10 $\mu g/m^3$, whereas in an urban environment the mass concentration typically ranges 10-1000 $\mu g/m^3$. Similarly, the particle number concentration gives the number of particles per unit volume of air and is given in number/cm^3.

Another important measure of atmospheric composition is the mixing ratio C_x of a chemical species X. The mixing ratio is defined as number of moles per mole of air and gives the atmospheric concentration of X [1]. The most abundant gas in the atmosphere is nitrogen (N_2). With a mixing ratio of C_{N_2}=0.78 [mol/mol], it makes up 78% of the molecules in the atmosphere. Nitrogen is followed by oxygen (O_2, 21%) and argon (Ar, 0.93 %) [1]. These mixing ratios exclude the water vapor mixing ratios, since water evaporates and condensates constantly resulting in large variations. Gases, other than N_2, O_2, Ar and H_2O, appear at very low concentrations in the atmosphere and are called trace gases. Despite their small abundance, trace gases are of major importance for the global climate and are given in units of parts per million (ppm, 10^{-6}) or parts per billion (ppb, 10^{-9}).

2.3 Climate impact

An aerosol in the atmosphere can not only affect local weather, visibility or population health (e.g. the great smog of London, 1952), but also has a significant influence on global atmospheric processes such as global warming.

However, clouds and aerosols contribute to the largest uncertainties in estimates of Earth's changing energy budget [11]. This energy budget describes the balance between the incoming solar radiation the Earth receives and the energy it radiates back into space. A perturbation in this balance results in a global temperature change, which can be either positive or negative, resulting in a net warming or cooling effect, respectively. The magnitude of this radiation balance perturbation, exerted by a certain substance, e.g. CO_2 or aerosol particles, is commonly expressed in a term called radiative forcing (RF). Radiative forcing, as it is formally defined in a previous Intergovernmental Panel on Climate Change (IPCC) report [12], represents the change in net downward radiative flux (shortwave and longwave, in W/m^2) at the tropopause after allowing for stratospheric temperatures to readjust to radiative equilibrium, while holding other state variables (e.g. tropospheric temperatures, cloud coverage) fixed at the unperturbed values [12]. A correct parametrisation of clouds and aerosols is needed to develop accurate climate models and prognosis [3]. The effects on Earth's climate from an atmospheric aerosol can be both direct and indirect.

The direct effect occurs, when aerosol particles scatter or absorb incoming solar radiation, thereby altering Earth's reflectance (albedo). An increase in Earth's albedo due to scattering has a net cooling effect on Earth's surface since a larger amount of solar radiation is back scattered into space. The amount of sunlight scattered by aerosol particles depends on the particle size (i.e. the scattering is maximized when the particle diameter equals the photon's wavelength) and the depth of the aerosol layer [1]. While, aerosol scattering tends to cool the climate systems, the opposite holds for aerosol absorption [11]. However,

most aerosol particles, except Black Carbon (soot), mainly scatter light.

As mentioned in section 2.1, aerosol particles can undergo heterogeneous nucleation to form clouds. A high density of cloud condensation nuclei leads to the formation of many but small cloud droplets, which brighten the cloud and reflect more solar radiation. This phenomenon is called the indirect effect and is most effective above dark surfaces such as oceans.

Hence, aerosols impact the climate by direct negative radiative forcing and by serving as cloud condensation nuclei. However, determining the effective climate impact of aerosols is complex and undetermined, which is mainly due to the large uncertainties in the relative impact of either natural or anthropogenic aerosols. Detailed aerosol particle observations have only existed for $\sim$20 years such that the aerosol concentrations during pre-industrial conditions are unknown and can only be assumed through model simulations which need to be accurate. Therefore, it is vital to understand the details of DMS oxidation and how it contributes to secondary aerosol formation, in order to improve our climate model projections.

2.4 DMS

Globally, the main natural source of sulphur to the atmosphere is the oxidation of ocean emitted dimethyl sulfide (DMS), known under the chemical formula CH_3SCH_3. This chemical compound is released by phytoplankton at the ocean surface and oxidises in the atmosphere to various sulfur-containing compounds, such as sulfur dioxide (SO_2), methanesulfinic acid (MSIA), dimethyl sulfoxide (DMSO), methanesulfonic acid (MSA) and sulfuric acid (H_2SO_4).

All these oxidation products of DMS contribute to secondary aerosol formation over the ocean, either by nucleation (H_2SO_4), condensation onto existing aerosol particles (H_2SO_4, MSA) or by dissolution in cloud droplets followed by aqueous-phase oxidation (SO_2, MSIA, DMSO) leading to sulfate or MSA. In the CLAW hypothesis, proposed by Charlson et al. in 1987 [2], this process was suggested and filled the missing link in the global atmospheric sulphur budget.

The resulting aerosol particles serve as cloud condensation nuclei over the open ocean. With 70% of Earth's surface covered by oceans, that have a generally low reflectance, marine DMS aerosols have a great impact on the global climate through strong negative radiative forcing and altering marine cloud properties [3]. In the atmosphere DMS predominantly reacts with the hydroxyl radical (OH) and also the nitrate radical (NO_3). These two radicals are sinks for DMS since their reaction with DMS removes it from the atmosphere.

The production of OH in the atmosphere is influenced by several chemical reactions and happens via the oxidation of water (H_2O) involving a singlet state excited oxygen ($O(^1D)$):

$$H_2O + O(^1D) \longrightarrow 2OH$$

The high energy $O(^1D)$ stems from the photolysis reaction (a reaction with light, *hν*) of ozone (O_3). However, the photolysis of nitrogen dioxide (NO_2) produces oxygen (O) which in turn is needed to produce ozone. Therefore, the amount of photolysis reactions of NO_2, in explicit the photolysis rate of NO_2, affects the OH concentration in the atmosphere and is directly correlated to the UV-light intensity. Further, this means the OH concentrations are very low at night time since there is no $O(^1D)$ to perform the reaction above.

The OH reactions with DMS take place in two ways via an abstraction (an H atom is abstracted) and addition (the OH radical is added as a -OH functional group) pathway:

$$CH_3SCH_3 + OH \longrightarrow CH_3SCH_2 + H_2O \qquad \text{(abstraction)}$$
$$CH_3SCH_3 + OH + M \longrightarrow CH_3S(OH)CH_3 + M \qquad \text{(addition)}$$

Through multiple gas-phase reactions the stable chemical components described above are formed, but their exact parametrisation and further reactions are yet to be understood.

The addition pathway mainly leads to the formation of sulfuric acid (H_2SO_4) which is a key precursor for particle formation through nucleation; the abstraction path mainly leads to the formation methanesulfonic acid (MSA) which influences particle growth through condensation. The branching ratio of both gas-phase reactions above is strongly temperature dependent [13]. Furthermore, studies have shown that aqueous-phase reactions of DMS also contribute to the secondary aerosol formation [3]. However, we still lack detailed knowledge about the DMS multi-phase chemistry, which not only affects the production of the secondary aerosols but increases the uncertainty in global climate models.

In January 2020 Veres et al. [7] reported an atmospheric observation of the stable oxidation product of DMS called hydroperoxymethyl thioformate (HPMTF), which was perviously only observed in laboratory flow tube experiments on DMS by Berndt et al. [14]. The lack of knowledge about this oxidation product poses additional difficulties on determining an accurate DMS oxidation scheme.

2.5 This work

This thesis work investigates the DMS oxidation and aerosol formation in three different set-ups. Firstly, the Butanol-OH experiments review the general chamber conditions concerning UV-light intensity and relative humidity. The results will be used to investigate if any changes are need to be done upfront the laboratory DMS experiments.

Secondly, the first smog chamber experiments on DMS oxidation are simulated with a series of sensitivity tests including the recently discovered DMS oxidation product Hydroperoxymethyl thioformate (HPMTF) (Wu et al. [15], Berndt et al. [14], Veres et al. [7]) and modified oxidation schemes. Here, the influence of the oxidation products on the secondary aerosol formation is studied in a chamber setup.

Thirdly, an atmospheric setup is explored to investigate DMS gas-and aqueous-phase chemistry in the presence of halogen species emitted over the ocean. The previous two

experimental set-ups mainly concern the gas-phase chemistry of DMS, however, studies such as Barnes et al. [4] and Hoffmann et al. [3] show that neglecting aqueous-phase reactions of DMS leads to a wrong estimation of the production amount (product yield) of MSA and the aerosol precursor gas SO_2, which oxidises into sulfuric acid H_2SO_4. Ignoring the aqueous-phase reactions supposedly leads to an overestimation of the H_2SO_4 aerosol concentration and the number of cloud condensation nuclei (CCN). This would result in a higher cloud brightening effect than in the case of including the aqueous-phase reactions, meaning that without the aqueous-phase reactions, global climate models may overestimate the indirect effect of DMS-aerosols.

The atmospheric simulations investigate if ADCHAM can capture a similar impact to Hoffmann et al.[3] of halogens and aqueous-phase cloud processes on the DMS oxidation, as well as model the detailed interaction processes which lead to atmospheric secondary aerosol formation from DMS.

3 Method

3.1 Box model

The concentration of a chemical species X in the atmosphere is influenced by four different processes: the emission to the atmosphere (e.g. biogenic or anthropogenic), the chemical reactions in the atmosphere which increase or decrease the concentration, the transportation of the species in the atmosphere (e.g. due to wind), and its dry- or wet-deposition (see figure 3). To integrate all these processes and investigate their interaction, mathematical model systems are a useful tool to transform the complexity of the real atmosphere into a analytical and numerical solvable framework [8].

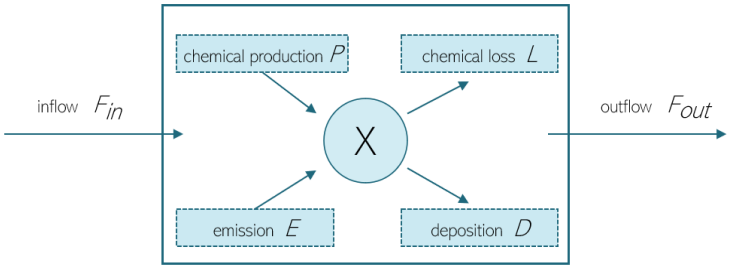

Figure 3: The box model system for a chemical compound X. The chemical production P, the emission E and inward transport F_{in} act as sources of X, whereas the the remaining are sinks of X.(Reproduced from Fig. 3-1 in *Introduction into Atmospheric Chemistry* [1])

The simplest type of model is the one-box model shown in figure 3 which describes the concentration of the species X in a certain area of simulation (domain). Here, all variables and conditions are assumed to be homogeneously mixed. The atmospheric domain could be a country, a city or the global atmosphere, in which case the transport of species into F_{in} and out F_{out} of the box would be equal to 0. From this box-model quantities such

as the lifetime of X, the loss- and source rate of X and the mass at a certain time can be calculated. The ADCHAM model used in this thesis to simulate secondary aerosol formation from DMS, is a one-box model.

3.2 AURA- smog chamber

When doing research on the atmosphere, smog chambers are a widely used tool since they allow to artificially control conditions and surroundings. The simulations investigated in this thesis rely on the smog chamber experiments done at Aarhus university, Denmark. The Aarhus University Research on aerosol (AURA) smog chamber allows for atmospheric simulations of the secondary aerosol particle formations following the oxidation of VOCs (such as DMS).

The AURA smog chamber consists of a Teflon bag in shape of a cuboid with a volume of about 5 m^3. This bag is suspended from a metal frame into a temperature controlled cold room with a temperature range of 257-299 K. In addition to a stainless steel inlet and outlet at opposite sides, the chamber has 24 UV-A/B (300-400 nm) lamps to vary the UV-light intensity [16].

All the chamber experiments where done by releasing the needed gaseous compounds into the Teflon bag and shining UV-light on them for a certain amount of hours. Meanwhile, a small amount of air was sucked out from the Teflon bag (at a rate of $\sim$ 4-6 L/min) to measure the particle size distributions and the compound concentrations. Further, the temperature and relative humidity was constantly monitored. The AURA experiments were run for 20 hours, however, after 13 hours a certain fraction of the remaining air in the smog chamber was extracted for filter sampling and off-line chemical analysis. The measurements of the DMS smog chamber experiments are used as reference for the ADCHAM simulations done in this thesis work.

3.3 ADCHAM

To simulate the smog chamber experiments on DMS oxidation and secondary aerosol formation the aerosol dynamics, gas- and particle-phase chemistry kinetic multi-layer model for chamber simulations (ADCHAM) [6] was used. As the name implies, this box-model is used to evaluate and design controlled experiments in a chamber environment, such as a smog chamber. Most importantly, the model gives insight into processes such as gas-phase chemistry, particle formations and aerosols dynamics which leads to better understanding of atmospheric aerosols.

The model structure of ADCHAM consists of 4 main building blocks: (1) a detailed gas-phase chemistry module, (2) an aerosol dynamics module, (3) a molecular cluster dynamics module and (4) a particle-phase chemistry module, shown in figure 4 below.

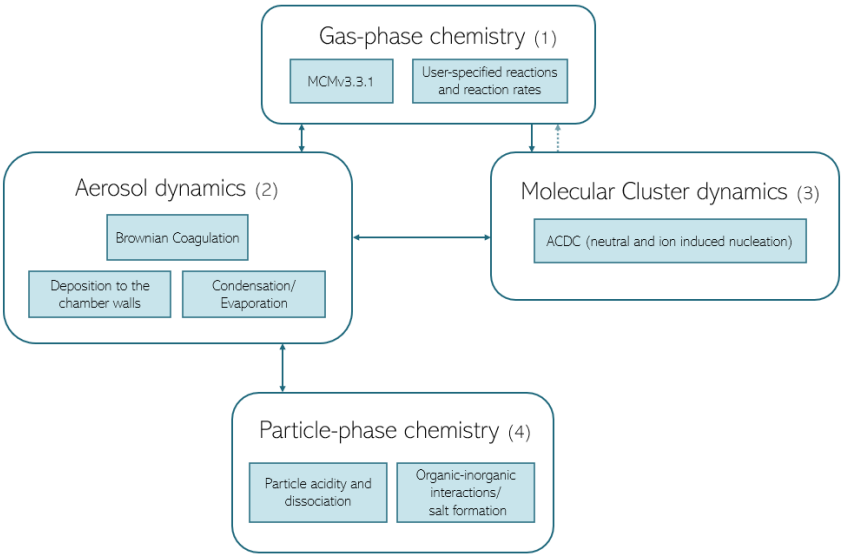

Figure 4: This figure shows the model structure of ADCHAM.

The gas-phase chemistry model (1) implements the detailed Master Chemistry Mechanism version 3.3.1 (MCMv3.3.1). This mechanism is widely used open access tool that describes gas-phase chemical processes for VOCs emitted to lowest region of the atmosphere. The MCMv3.3.1 in addition with a program that includes specified reactions and reaction rates (e.g. chamber wall losses, halogen chemistry from CAPRAM Halogen Module [5] and Hoffmann [3]), makes up the gas-phase chemistry model which is needed to compute the concentrations of the compounds involved in the study. The gas-phase chemistry is described by a coupled set of ordinary differential equations, one equation for each species, which is solved with the differential equation solver DLSODE. The DMS gas-phase chemistry scheme includes in total 174 species and 507 reactions. For the atmospheric model simulations the model also considers emissions of several VOCs, including Isoprene from the ocean. This gas-phase chemistry scheme in total comprises 812 species and 2546 reactions.

Further, the Aerosol dynamics model (2) includes Brownian coagulation, deposition of gases and particles to the chamber walls, as well as condensation and evaporation. The molecular cluster dynamics module (3) entails a Atmospheric Cluster Dynamics Code (ACDC) [17] which includes neutral and ion induced nucleation of sulfuric acid (H_2SO_4) and ammonia (NH_3). The nucleation rate (new particle formation rate) is calculated as the formation rate of molecular clusters reaching the size of 5 H_2SO_4 and 5 NH_3 molecules. These 10 clustered molecules make up 1 particle of the size of 1 nm.

The particle phase chemistry model (4) can simulate non-ideal mixing between organic and inorganic compounds and is closely related to the condensation algorithm and evaporation in (2). It takes in account the particle acidity and dissociation, organic-inorganic interactions and salt formation.

The original ADCHAM model also includes a kinetic multi-layer model which among other things describes the diffusion of compounds between particle surface and several

bulk layers (interior). However, in this work the kinetic multi-layer model was not used since the formed particles are considered to be liquid, well-mixed droplets such that there are no concentration gradients between the particle surface and particle bulk.

As mentioned before, the gas-phase chemistry for DMS stems from MCMv3.3.1 and Hoffmann [3], as well as selected halogen chemistry from Bräuer et al. [5]. However, the halogen chemistry is only of relevance in the atmospheric DMS simulations. Nevertheless, the oxidation to HPMTF, aqueous-phase reactions and halogen-DMS reactions still entail many uncertainties that will be investigated in the simulations below.

3.4 Butanol-OH experiments

In spring 2019, a total of 12 Butanol-OH experiments were done at the AURA smog chamber. Here, Butanol is released into the chamber and allowed to react in the presence of UV-light under conditions resembling atmospheric day-time. The main sink of Butanol, similar to DMS, is OH. However, the two compounds differ in their oxidation products and schemes such that the overall OH concentrations in the chamber will be influenced differently by these compounds and their oxidation products.

The Butanol-OH chamber experiments indicate that the OH concentrations and the butanol decays in the chamber are influenced by the relative humidity (RH), with higher RH generally leading to lower OH concentrations. This indicated dependence on the RH, results in an apparent shift in the UV-light intensity. However, during the experiments the OH concentration was not measured, but derived from the observed butanol decay. The aim of the ADCHAM simulations is to see which UV-light intensity is required in order for the model to reproduce the OH and Butanol data from the experiments, as well as investigate what causes the change in UV-light intensity through several sensitivity tests. Further, the results of the simulations can give insight into changes needed to be done for the general chamber set-up in the following DMS simulations.

The simulations concentrate on the experiments injected with an initial concentration of 20ppm of hydrogen peroxide (H_2O_2), which results in a total of 4 experiments. The H_2O_2 serves as a source of OH when being photolysed by the UV-light. The set-up conditions of the ADCHAM-model were done as close as possible to the chamber experiments, see table 1. Therefore, the NO_2-photolysis rate, which defines the UV-light intensity (see section 2.4), was set to 0.19 min^{-1}, as previously reported by Kristensen et al. [16], and the Butanol initial concentrations (see table 1) were chosen to match the experiment data.

Table 1: The ADCHAM model conditions for the Butanol-OH simulations

Experiment date	RH (%)	T (K)	[Butanol] (ppb)
2019-03-26	5	293	350
2019-03-28	55	293	380
2019-03-29	75	273	190
2019-04-01	70	258	510

The ADCHAM model was run for all four experiments and the resulting mean OH-concentrations and Butanol-concentrations were compared to the experimental data.

A total of four different sensitivity tests on the model were done to test its response compared to the experiment data. Firstly, the initial ozone concentration was changed from 1 ppb to 10 ppb. Secondly, the NO_2-photolysis rate was adjusted to account for its temperature dependence characterized by Kristensen et al. [16]. At full light intensity, the paper states the NO_2-photolysis to be 0.19 min^{-1} at 293 K and 0.09 min^{-1} at 258 K. Thirdly, the the initial concentration of Nitrogen dioxide NO_2 was varied between 0.1, 1 and 10 ppb.

Lastly, the effect of the chemical compound HONO, presumably released from the Teflon walls of the chamber, was investigated. A paper by Zador et al. [18] describes the OH production from HONO (at RH = 10-15 %) to be about a factor of two higher than that from the photolysis of 100 ppb ozone. Therefore, a HONO production rate was included in the simulation to investigate if it could account for the increased UV-light intensity.

3.5 Laboratory DMS experiments

The oxidation of DMS by OH radicals was studied at the AURA smog chamber, in a likewise manner to the Butanol-OH experiments described in the section above. During the course of two measuring campaigns, the DMS laboratory experiments aimed to quantify the properties of the formed secondary aerosol particles. This thesis work concentrates on simulating the first campaign which examines the DMS oxidation and secondary aerosol particle formation at low relative humidity, so called dry conditions.

As mentioned before, the ADCHAM model [6] used in this work already entails a detailed gas-phase chemistry mechanism including reaction pathways of DMS (MCMv3.3.1.1). Nevertheless, the DMS oxidation scheme has been extensively studied by Barnes [4], Bräuer [5], Hoffmann [3] and Veres [7], giving different representations for the oxidation mechanism which have to be evaluated against the laboratory experiments from AURA. The main focus in this work lies on finding the favourable representation for gas-phase DMS reaction mechanism and gain insight into how the DMS oxidation products methanesulfonic acid (MSA), methanesulfinic acid (MSIA), sulfuric acid (H_2SO_4) and hydroperoxymethyl thioformate (HPMTF) contribute to the formation and growth of aerosol particles during the smog chamber experiments. In the course of four different sensitivity tests, these above mentioned focus points are investigated.

From the first campaign mainly the two earliest DMS experiments were simulated of which the model set-up is shown in table 2. The two experiments only differ slightly, making them ideal to compare. The first experiment, different to the second, has no measured DMS concentration from the smog chamber experiment such that the modelled DMS concentration is to be seen as an estimate. Further, the particle mass formation from HPMTF and MSIA is very sensitive to the particle water content. Therefor, the model reads in the exact observed RH from the chamber during the simulation. Here, the RH increases from below 1 % to 5-12 % during the experiments.

Table 2: The ADCHAM model conditions for the DMS simulations

Experiment date	T (K)	[DMS] (ppb)	[H_2O_2] (ppm)	NH_3 (ppb)	[NO_2] (ppb)	[O_3] (ppb)
2018-04-05	293	200	20	1	1.3	1
2018-05-19	293	220	20	1	1.5	1

The first sensitivity test concerns the representation of the DMS gas-phase reaction scheme. The model representation from MCMv3.3.1.1 is evaluated against representation suggested from Barnes et al. [4]. In the MCM representation the DMS oxidation product MSIA can only react to form SO_2, whereas the Barnes representation includes additional reaction pathways allowing MSIA to form SO_2, MSA and sulfuric acid H_2SO_4. Each representation is used to simulate the laboratory experiment 2018-04-05 (see table 2) and evaluated against the experiment data.

The second sensitivity test regards wall losses of the DMS oxidation products MSIA and HPMTF. The ADCHAM model already includes the wall losses from H_2SO_4 and MSA. Both acids are categorized as strong meaning they lose a proton easily and are most likely lost to the chamber walls irreversibly at a rate of $\sim 2.4\text{x}10^{-3}$ s^{-1}. However, if HPMTF and MSIA are lost to the walls at a similar rate, the new particle formation will be most likely suppressed. The model was run with and without wall losses of MSIA (irreversible) and HPMTF (reversible).

The recently discovered DMS oxidation product HPMTF [7] brings further unknowns with it. The chemical compound could either be in hydrated or non hydrated form in the aqueous particle phase, meaning it either contains water in form of H_2O-molecules or not. A sensitivity test was done by changing the Henry's law coefficient, which describes the distribution of a certain compound (here HPMTF) between the air and liquid aerosol particles in the algorithm, corresponding to either the hydrated or non-hydrated form of HPMTF.

Further, a different gas-phase chemistry representation for the autoxidation of $CH_3SCH_2O_2$ and formation of HPMTF was tested. HPMTF is formed by the oxidation of DMS via the H-abstraction pathway. The compound $CH_3SCH_2O_2$ is the first oxidation product from the DMS-OH reaction via the H-abstraction pathway. Recent experiments (Berndt et al. [14]) indicate that $CH_3SCH_2O_2$ can undergo rapid intramolecular H-atom shifts and rapid uptake of oxygen molecules (O_2), so called autoxidation, in two steps. The stable end-product is HPMTF. The sensitivity test was conducted by either setting the autoxidation rate to 0 resulting in no HPMTF formation or increasing the rate compared to approximate values used by Veres et al. [7].

3.6 Atmospheric DMS tests

Previous studies such as Barnes et al. [4] and Hoffmann et al. [3] show that neglecting aqueous-phase reactions of DMS leads to a wrong estimation of the production amount (product yield) of MSA and the aerosol precursor gas SO_2, which oxidises into sulfuric acid H_2SO_4. The ADCHAM model used for the atmospheric DMS tests includes a total of

6 ideal cloud passages during a 72 hour simulation, displaying similar environmental conditions as in Hoffmann et al. [3], which is used as reference for the ADCHAM simulations. The aim of including the cloud passages is to test if ADCHAM can capture the impact of the cloud aqueous-phase processes on the DMS oxidation and oxidation products, as well as to study the aerosol formation under atmospheric relevant conditions.

In the article written by Hoffman et al. [3] it is indicated that during cloud passages the aqueous-phase reactions dominate the oxidation of DMS and significantly lower the gas-phase concentrations of OH and certain halogen species. The main oxidation path of DMS during cloud passages should be via ozone O_3 due to aqueous-phase reactions taking over the gas-phase reactions.

The first sensitivity test investigates if the ADCHAM box-model can capture the DMS-concentration simulated by Hoffmann et al. [3] during an ideal cloud-passage sensitivity run without halogens. The ADCHAM model was set-up as close as possible to the Hoffmann set-up, including most of the chemical reactions, reaction- and emission-rates and the initial concentration implemented by Hoffmann et al. [3]. A total of 4 different simulations of the DMS concentration are done, with variable sun light intensity corresponding to a maximum (noon-time) NO_2-photolysis rate, $J(NO_2)$, to see which UV-light intensity is needed to match Hoffmanns DMS concentration trend. The used values of $J(NO_2)$ are: 0.09 min^{-1}, 0.23 min^{-1}, 0.90 min^{-1} and 1.80 min^{-1}.

Moreover, Hoffmann states that a higher DMS emission results in higher particulate mass but not necessarily in a higher aerosol number concentrations. It is expected that in ADCHAM a higher DMS emission rate results in a slight increase in the number concentration, but most likely the number concentration is more sensitive to the ammonia concentration. The ACDC code in ADCHAM (see section 3.2) simulates the formation and growth of NH_3-H_2SO_4 molecular clusters, of which the resulting particles then contribute to the particle number concentration. A higher DMS emission rate would mean more sulfuric acid molecules, while a higher ammonia concentration would result in more ammonia molecules. This poses the question which of the two is the limiting factor on the new particle formation rate, which reflects on the particle number concentration. Therefore, the second sensitivity test simulates the new particle formation rate (nucleation rate) for three different DMS emission rates ($E_{DMS} = 6.18 \cdot 10^8$, $6.18 \cdot 10^9$, $6.18 \cdot 10^{10}$ cm^{-2} s^{-1}) while keeping the ammonia emission constant ($E_{NH_3} = 1 \cdot 10^9$ cm^{-2} s^{-1}), and for three different ammonia emission rates ($E_{NH_3} = 1 \cdot 10^8$, $1 \cdot 10^9$, $1 \cdot 10^{10}$ cm^{-2} s^{-1}) while keeping the DMS emission constant ($E_{DMS} = 6.18 \cdot 10^9$ cm^{-2} s^{-1}). All test have no initial concentration of ammonia.

During the previous laboratory experiments (see sections 3.4 and 3.5), the DMS oxidation was not expected to be influenced by reactions involving halogens, since the halogen concentrations were anticipated to be negligible low during these experiment. However, in marine environments the halogen chemistry becomes more important. In the following sensitivity tests the ADCHAM model is used to investigate and quantify the impact of halogen reactions on the DMS aerosol formation.

The halogen chemistry in ADCHAM was set-up to again follow the reactions and reactions rates implemented by Hoffmann et al. [3]. The ADCHAM model was run with an without halogen emissions to test the impact of halogen-DMS reactions on the aerosol mass of the oxidation products MSA and sulfuric acid (H_2SO_4). Then the sink fluxes of DMS were investigated, displaying how much of DMS reacts with the halogens, chlorine (Cl) and bromine oxide (BrO), as well as OH. Both simulations were done with the idealized cloud passages to look at the combined influence of halogens and the multi-phase reactions on the DMS oxidation and secondary aerosol formation.

4 Results and Discussion

4.1 Butanol-OH experiments

The simulations shown in figure 5 agree reasonably well under high humidity conditions, but differ under dry conditions as shown in figure 5a which displays the simulation for the first experiment (26-03-2019). Here, the model substantially underestimates the Butanol decay, as well as the experimentally estimated OH-concentration in the chamber shown in table 3. For the model to fit the measured Butanol concentration the UV-light intensity would need to be doubled resulting in a NO_2-photolysis rate of 0.38 min^{-1}.

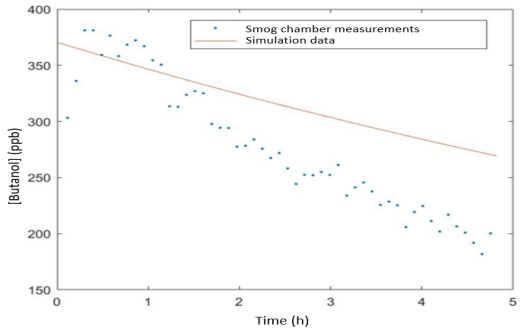

(a) Simulation for the experiment 2019-03-26 with T=293K and RH=5 %. (dry conditions)

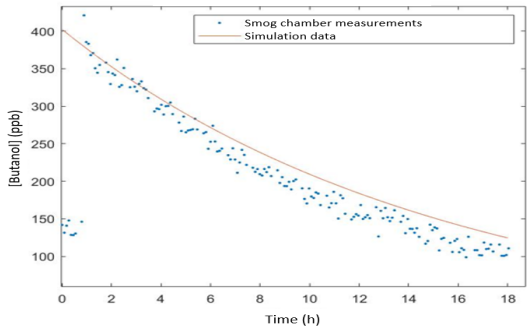

(b) Simulation for the experiment 2019-03-28 with T=293K and RH=55 %. (humid conditions)

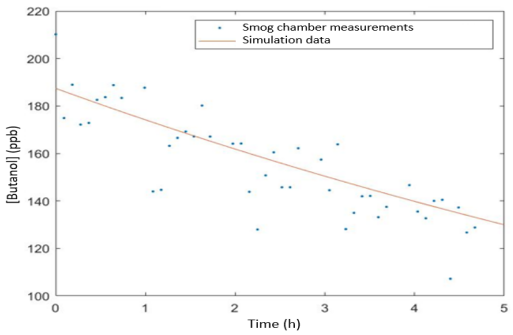

(c) Simulation for the experiment 2019-03-29 with T=273K and RH=75 %. (humid conditions)

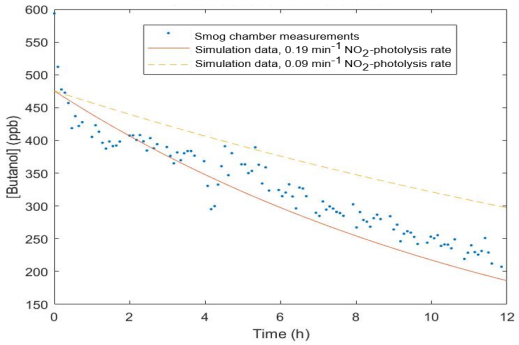

(d) Two simulations for the experiment 2019-04-01 with T=258K and RH=70 %. (humid conditions). The simulations differ in their photolysis rate.

Figure 5: The ADCHAM model simulations of the measured Butanol concentration for the four different experimental set-ups shown in table 1.

The first sensitivity test of changing the initial O_3 concentration had no major effect on the model performance. The results of the second sensitivity test are shown in figure 5d. Here, the figure 5d compares the measured chamber concentration of Butanol to two simulations which differ in their UV-light intensity as indicated by the two different NO_2-photolysis rates, $J(NO_2)$.

As described in the method section, in this simulation (5d) the set UV-light intensity corresponding to a NO_2-photolysis rate of $0.19 min^{-1}$ was reduced to $0.09 min^{-1}$ due to observations by Kristensen et al. [16], in which a colder temperature in the chamber decreases the photolysis rate. When looking at the two simulations, the higher photolysis rate matches the measured butanol concentration better indicating a need for a doubled UV-light intensity. In addition, the lower photolysis rate underestimated the OH-concentration estimates in the chamber to a large extent, while the doubled UV-light intensity ($J(NO_2)$=$0.19 min^{-1}$) matches the OH-concentration estimates fairly well (see table 3).

Table 3: [OH] concentrations in comparison and absolute humidity ([H_2O]) in molec/cm^3

$J(NO_2)$	T (K)	Experiment date	[OH] (Experiment)	[OH] (Simulation)	[H_2O]
$0.19\ min^{-1}$	293	2019-03-26	$4.82 \cdot 10^6$	$2.128 \cdot 10^6$	$2.82 \cdot 10^{16}$
	293	2019-03-28	$2.52 \cdot 10^6$	$2.109 \cdot 10^6$	$2.82 \cdot 10^{17}$
	273	2019-03-29	$2.49 \cdot 10^6$	$2.296 \cdot 10^6$	$1.20 \cdot 10^{17}$
	258	2019-04-01	$1.95 \cdot 10^6$	$2.160 \cdot 10^6$	$4.21 \cdot 10^{16}$
$0.09\ min^{-1}$	258	2019-04-01	– " –	$1.039 \cdot 10^6$	– " –

The third sensitivity test on changing the initial concentration of NO_2 had again a negligible effect on the simulations. However, the addition of the HONO production rate from the chamber walls resulted in a 1-2% change in the OH-concentrations. Still, this cannot explain the observed large variation in the butanol decay rate, which is a proxy for the OH-concentration in the chamber.

To do further investigations, the water content of the air, absolute humidity, in the chamber was calculated (see table 3). The absolute humidity ([H_2O] in molecules/cm^3) regulates the gas-phase chemical reactions and may influence the gas-phase kinetics (collision rates between H_2O and other molecules), which the RH should not. However, looking at the model simulations the influence of the absolute humidity does not support the change in the UV-light intensity. This, together with the model simulations, indicates that the impact of the RH on the OH-concentrations are not related to the gas-phase kinetics involving H_2O molecules. Instead it may be related to changed chamber wall properties.

It may be that the properties of the chamber walls change over time between high and low RH. As an example, the Teflon walls could potentially become opaque during the high humidity experiments such that the water condenses onto the chamber walls as they are colder than the interior of the chamber. Less opaque chamber walls at dry conditions would then allow for more UV-light to come through the walls, which would account

for the increase in OH-concentrations under dry conditions. Nevertheless, the reason and process of the changed chamber wall properties is still unknown. Unlike the experimental data, the model shows no signs of sensitivity to the RH and there is no chemical explanation to the observed RH dependence on the Butanol decay and OH-concentrations. Hence, for the below simulated DMS experiments at 293 K an UV-light intensity corresponding to a NO_2-photolysis rate of $0.19 min^{-1}$ was used.

4.2 Laboratory DMS experiments

The concentration of ammonia (NH_3) in the chamber is one of the largest uncertainties in the model and experimental set-up. The NH_3 could be leaked through the Teflon bag from outside or released into the chamber by evaporation from the Teflon walls. The ADCHAM model results on new particle formation, as well as the secondary aerosol formation from MSA, are highly sensitive on the NH_3 concentration.

This sensitivity leads to the hypothesis that the new particle formation and mass formation are controlled by the NH_3 concentration and relative humidity in the chamber. Without NH_3 no new particles can be formed from NH_3-H_2SO_4 clusters, meaning there are no sites for condensable gases, such as MSA, to form particles on. A fixed concentration of 1 ppb NH_3 was used for the ADCHAM model simulations of the DMS laboratory experiments. This fixed concentration may represent conditions where the gas-phase NH_3 concentrations is in a steady-state equilibrium between loss to the particle phase and releases from the chamber walls. For future investigations, the NH_3 concentration could be set to change during the course of the experiments. However, since the NH_3 concentration was not measured during the experiments, this can only be investigated with model sensitivity tests.

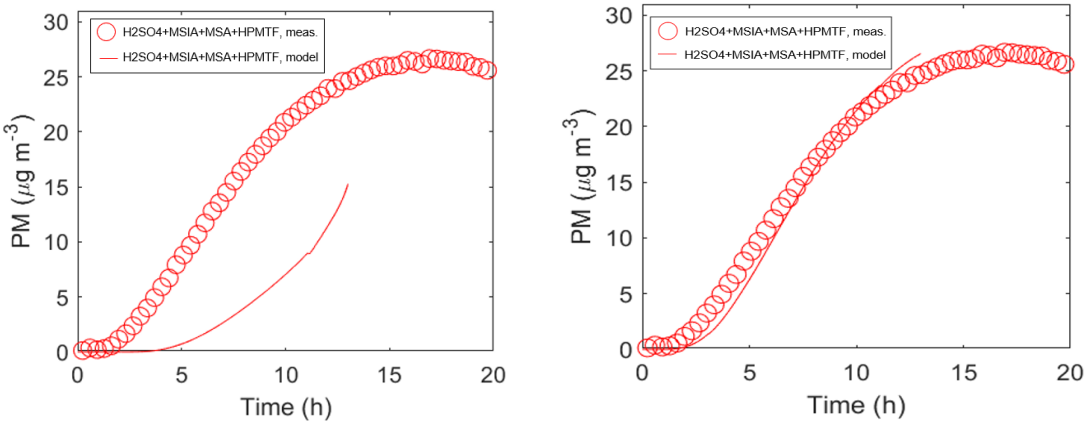

(a) MCM representation

(b) Barnes representation

Figure 6: ADCHAM model simulations of the H2SO4, MSA, MSIA and HPMTF particle mass measured in experiment 2018-04-05. Each figure displays one of two DMS gas-phase representations, 6a) MCMv3.3.1.1 and 6b) Barnes.

The figure 6 above shows two ADCHAM model simulations of the H_2SO_4, MSA, HPMTF and MSIA particle mass on the experiment 2018-04-05. An Aerodyne High-Resolution Time-of-Flight Aerosol Mass Spectrometer (HR-ToF-AMS, Aerodyne Research Inc., Kristensen et al. [16]) was used to obtain the particle mass during the smog chamber experiments. Each simulation corresponds to one of two different representations of the DMS gas-phase reactions schemes, (a) MCMv3.3.1 and (b) Barnes [4]. As described in the method section, in the MCM representation the DMS oxidation product MSIA can only oxidize into sulfur dioxide, while in the Barnes representation MSIA has additional reaction pathways leading to not only SO_2, but also H_2SO_4 and MSA. The difference in reaction pathways impacts the aerosol particle mass, such that the ADCHAM simulation are used to determine a favourable reaction scheme. The simulations below are compared to the observed particle mass from the smog chamber.

After ∼13 hours a large fraction of the remaining air in the chamber was removed for filter sampling and off-line chemical analysis. Therefore, only the first 13 hours of the simulation are compared to the measured particle mass. The simulations indicate a strong confidence in the Barnes representation of the DMS gas-phase reaction scheme, since the MCMv3.3.1.1 representation does not seem to capture the measured particle mass as well.

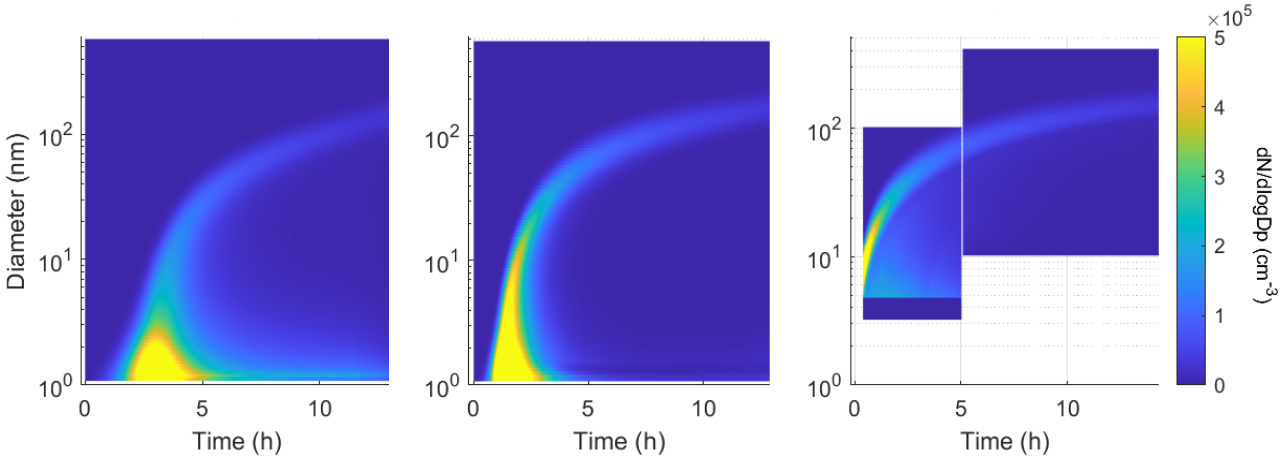

(a) MCM representation **(b)** Barnes representation **(c)** measured particle number

Figure 7: ADCHAM model simulations of the particle number size distribution in two different DMS gas-phase representations (7a,7b) compared to the obtained particle number in experiment 2018-05-04 (7c).

The same trend as in the particle mass is visible in the ADCHAM particle number simulations shown in figure 7. Here, the simulations of the particle number (see figure 7a,7b) are compared to the observed particles in the chamber (see figure 7c). The chamber measurements were done with a scanning mobility particle sizer (SMPS) system [16], which is able to measure particles in the range of 4-1000 nm with sampling times of about 30 s. The particle number modelled in the MCMv3.3.1.1 representation underestimates the initial density of new particle formation, whereas the Barnes representation seems to capture this density fairly well, including the resulting particle growth to approximately 100 nm. With the additional MSIA reaction pathways given in the Barnes representation, the

MCM representation may be too simplistic such that all following sensitivity tests were conducted with the Barnes representation.

The investigation concerning if HPMTF occurs in a hydrated or non-hydrated form only showed a minor difference on the model simulation of the combined H_2SO_4, MSA, MSIA and HPMTF particle mass. The contribution of HPMTF in its hydrated form was about a factor of 10 higher, but was still negligible for the total aerosol mass. This shows that HPMTF seems to only have a very small contribution to the total particle growth from DMS-oxidation products. The reason behind this limited contribution could be simulated reversible wall losses and relatively high volatility of HPMTF. Despite the small difference between the two forms, the hydrated form was chosen for further simulations.

Adding the wall losses of both HPMTF and MSIA to the model, largely suppressed the aerosol particle mass of H_2SO_4, MSA, HPMTF and MSIA. The only reasonable and good configuration to fit the measurements resulted in only allowing the reversible wall losses from HPMTF. Other configurations, such as wall losses from only MSIA or non of the two, resulted in numerical instability and vast fluctuations in the particle mass. This indicates that the model time step would have needed to be shortened in order to handle the reversible uptake of HPMTF towards the particle phase in these simulations. However, since the observations indicate that the HPMTF was not contributing significantly to the secondary particle mass formation during the experiments, it seems reasonable to consider that most HPMTF was lost to the chamber walls during the experiments.

For the different gas-phase chemistry representation of the autoxidation of $CH_3SCH_2O_2$ and subsequent formation of HPMTF different magnitudes of the autoxidation rate were tested. Increasing the set value suggested from Veres et al. [7] by a factor of 10 showed a drastic increase in the ozone (O_3) concentration in the chamber and suppressed the particle mass. Setting the autoxidation to 0, showed the opposite effect but less radical. Since the best configuration for the autoxidation rate seemed to be the initial value, the so far gathered model parametrisation shown in figure 8a (Barnes representation, only reversible wall losses from hydrated HPMTF, initial autoxidation rate from Veres et al. [7]) was used to simulate the second experiment 2018-05-19 shown in figure 8b.

The second experiment has the advantage of having observations of the DMS concentration in the chamber. However, the configuration gathered in previous sensitivity tests on experiment 2018-04-05 did largely overestimate the particle mass of H_2SO_4, MSA, HPMTF and MSIA in the second experiment 2018-05-19 as shown in figure 8.

Despite having nearly the same initial conditions, the reason for the difference in particle mass could be the relative humidity in the chamber. During the course of the second experiment the observed RH reaches 10-12 % instead of 5-6 % measured during the first. As previously hypothesised, the relative humidity influences the particle mass formation from MSA. In addition, the increase in relative humidity could imply that more humid air from outside the chamber was leaking into the Teflon bag during the second experiment. Since the model reads in the measured RH from the chamber, the RH sensitive particle and mass contribution from MSA could be overestimated, leading to an overall increased

particle mass in the simulation for the experiment 2018-05-19.

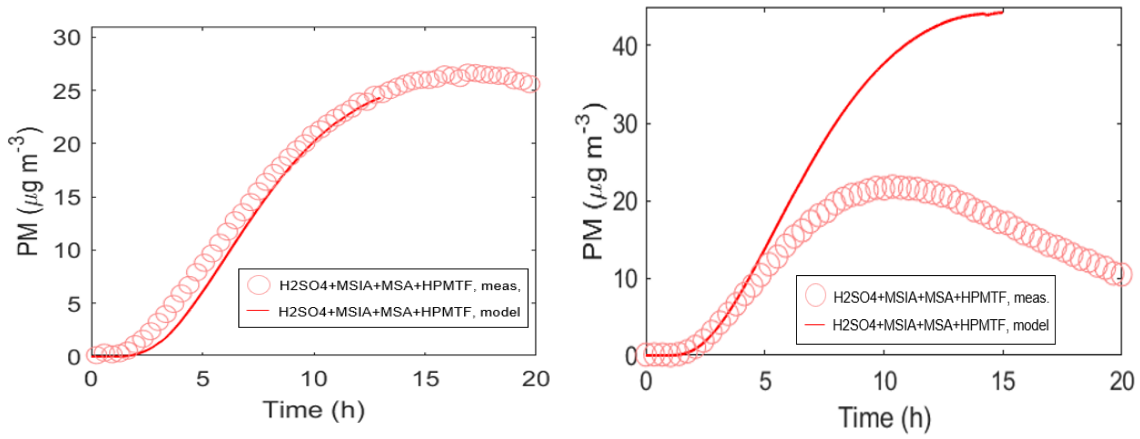

(a) Experiment 2018-04-05 **(b)** Experiment 2018-05-19

Figure 8: ADCHAM model simulations of the H2SO4, MSA, MSIA and HPMTF particle mass measured in the two smog chamber experiments investigated. The model parametrisation includes the Barnes representation, only reversible wall losses from hydrated HPMTF and initial autoxidation rate gathered from Veres et al. [7].

For the second experiment, multiplying the autoxidation rate by a factor of 100 made simulations fit the data fairly well, since a higher autoxidation suppresses the particle mass simulation. To decrease the ozone concentration, which increase is a result of the higher autoxidation rate, the NO_2 was set to 1.5 ppb such that it fits the measurements.

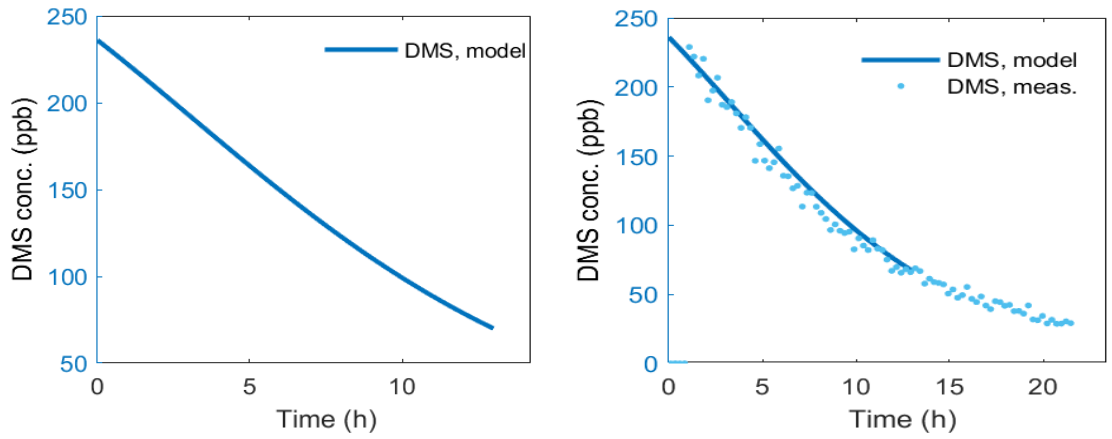

(a) Experiment 2018-04-05 **(b)** Experiment 2018-05-19

Figure 9: The ADCHAM simulated DMS concentration for both experiments. The chamber DMS concentration was only measured during second experiment 9b

The figure 9 shows the simulated DMS concentration for both experiments. Here, ADCHAM model set-up corresponds to the final version gathered in the sensitivity tests above. The second experiment 2018-05-19 in figure 9b compares the measured DMS concentration to the ADCHAM simulation, which captures the DMS decay very well. During

first experiment, the DMS concentration in the chamber was not measured, such that figure 9b only shows the simulation. However, since the two experimental set-ups are similar, the first experiment is assumed to display the DMS decay fairly well. The agreement of ADCHAM with the measurements indicates that the UV-light intensity (NO_2- photolysis rate of 0.19 min^{-1}) chosen from the Butanol-OH experiments seems to be reasonable for these dry experiments.

All in all, the sensitivity tests indicate a negligible contribution of HPMTF to the secondary aerosol formation, and that it is most likely lost to the chamber walls. Further, the reaction pathways leading to the HPMTF formation tend to suppress the net secondary aerosol formation from DMS. In addition, the autoxidation rate which results in the formation of HPMTF may be higher than predicted by Veres et al. [7]. The particle formation from MSA is mainly influenced by the relative humidity and ammonia concentration. However, the ammonia concentration remains uncertain in the chamber. The oxidation product MSIA has a too weak acid strength to contribute to the particulate phase at dry conditions. In general, ADCHAM model can capture the particle mass formation fairly well with the parametrsiation suggested above, but can not predict the particle nitrate content measured from the chamber experiments, which needs further investigations.

4.3 Atmospheric DMS tests

The ADCHAM simulations done to investigate the secondary aerosol formation from DMS under atmospheric relevant conditions are directly compared to a previous study done by Hoffmann et al. [3]. The simulations in Hoffmann indicate an increased importance of Halogen reactions and aqueous-phase reactions on the DMS oxidation, i.e. neglecting these reactions leads to a wrong estimation of the total DMS aerosol. A inaccurate estimation of the total particle number and mass of DMS aerosols poses a large uncertainty in climate models. The ADCHAM simulations are used to investigate the detailed processes of the aqueous phase and halogen reactions on the DMS oxidation, as well as see if the model can capture similar results and implications as in Hoffmanns work.

The results of the first sensitivity test, concerning the UV-light intensity, are shown in the figure 10 below. When applying solar radiation intensity corresponding to a maximum noon-time NO_2-photolysis rate of $J(NO_2) = 0.23\ min^{-1}$, the ADCHAM simulation of the DMS concentration shows nearly the same trend as the without-halogen-emission simulation done in Hoffmann et al. [3], which did not explicitly state the UV-light intensity. This indicates that the initial photolysis rate in the model ($J(NO_2) = 0.90\ min^{-1}$, red curve figure 10) may be about a factor of 4 times too high.

Further, the figure shows an anti-correlation between the amount of UV-light intensity and the DMS concentration. The higher the NO_2-photolysis rate, the lower the DMS concentration, and the more fluctuations in the concentration. In addition, it seems like a lower photolysis rate decreases the change of DMS concentration during cloud passages. Since the blue curve in figure 10 shows the best agreements with Hoffmann, the following atmospheric DMS tests were done at $J(NO_2) = 0.23\ min^{-1}$.

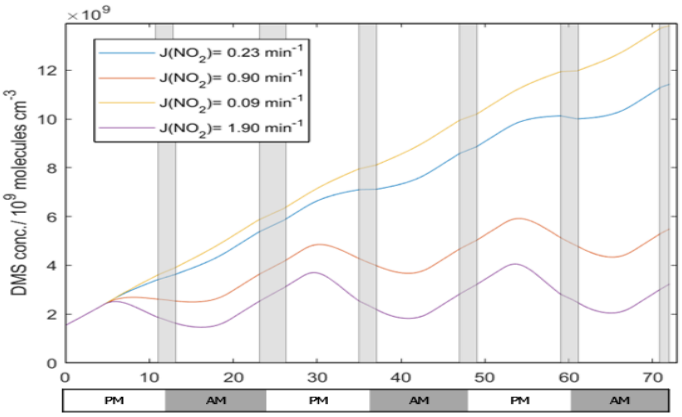

Figure 10: The DMS concentration for different UV-light intensities given by the value of NO_2-photolysis rate, $J(NO_2)$. The grey shaded areas display the cloud passages during the simulation.

In Hoffmann et al.[3] it is stated that a higher DMS emission rate does not necessarily lead to a higher particle number (PN) concentration, which the ADCHAM simulations disagree with. In table 4 below, it is shown that the ADCHAM simulated particle number increases at higher DMS emissions rates. Further, the figure 11 shows two simulations of the nucleation rate which describes the number of new particles formed per $cm^3 \cdot s$. As mentioned before, the particles are formed through the ACDC code (see section 3.2) by gradually growing clusters to the size of 5 ammonia (NH_3) molecules and 5 sulfuric acid (H_2SO_4) molecules such that they form a particle of the size of 1 nm. The nucleation rate is plotted with a base 10 logarithmic scale on the y-axis and a linear scale on the x-axis to make it easier to compare the different rates.

Table 4: Total aerosol PM and PN concentration at the end of the simulations in fig.11A

	$E_{DMS} = 6.18 \cdot 10^{10}$	$E_{DMS} = 6.18 \cdot 10^{9}$	$E_{DMS} = 6.18 \cdot 10^{8}$
total PN (cm^{-3})	1969	334.8	83.3
total PM ($\mu g/cm^3$)	3.379	1.71	1.54

The sub figure 11A displays the simulated nucleation rate for different DMS emission rates, while the sub figure 11B shows the same but for different NH_3 emission rates. Since the NH_3 emission rate is relatively high, this sensitivity test probably resembles the atmospheric conditions in coastal areas more than over remote ocean regions far from land.

The figure 11B shows a positive correlation between the number of particles formed and the magnitude of NH_3 emissions. In contrary, the nucleation rate at the high E_{DMS} (fig. 11A) decreases towards the end of the simulation compared to the runs with lower E_{DMS}. During the high E_{DMS} run more particle mass and more particle surface area are formed (table 4), resulting in larger condensation sinks of NH_3 to the existing particles. This means, even though the DMS emission is higher, the nucleation rate decreases. In general, this indicates that the new particle formation rate is primarily limited by strong bases, e.g. NH_3 and not the DMS emissions.

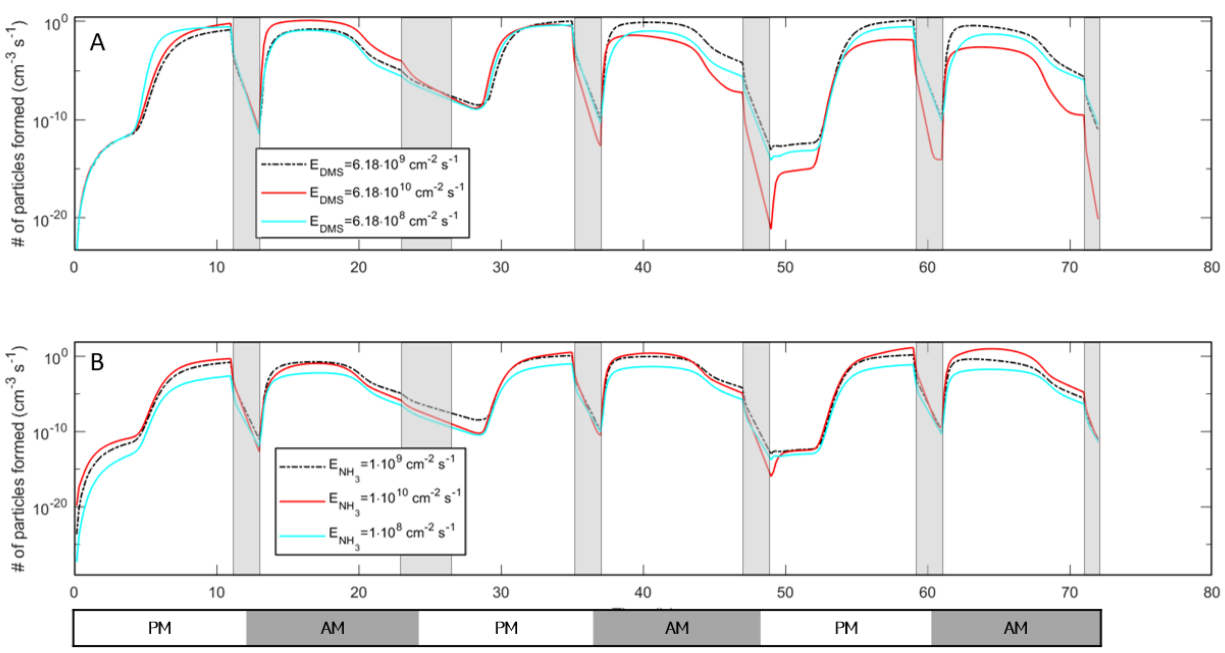

Figure 11: The ADCHAM simulation for the nucleation rate with ideal cloud passages shown as grey shaded areas. In the sub figure A the DMS emission rate was varied at a constant ammonia emission, while the opposite holds for sub figure B. In both figures the black, dash dotted line displays the exact same simulation.

The following simulations investigate the impact of halogen-DMS reactions and aqueous-phase reactions on secondary aerosol formation and oxidation of DMS under atmospheric conditions. The figure 12 below shows a comparison of the total particulate aerosol matter (PM) from MSA and H_2SO_4 for a simulation with or without Halogen emission (Hoffmann et al. [3]). The ADCHAM simulation displays a definite underestimation of the PM for both oxidation products of DMS when neglecting halogen-DMS reactions, indicating that atmospheric simulations without halogen emissions lead to underestimated product yields of MSA and sulfuric acid. The increase of aerosol particle mass from halogen emissions could be explained through a higher OH concentration , which is related through the effect of halogens enhancing the ozone degradation in the atmosphere (ozone depletion).

Further, the figure 13 below shows the gas-phase sink fluxes of DMS which describe how much DMS reacts with the displayed compounds; hydroxyl radicals (OH), chlorine (Cl) and bromine oxide (BrO). The stacked area plot shows that a significant amount of DMS reacts with the halogens. During clouds phases the DMS gas-phase sink fluxes increase slightly, while during the night times the sink fluxes almost completely diminish due to low concentrations of the OH, Cl and BrO at night times.

In Hoffmann et al., the effect of the cloud processing is more substantial which may be due to higher Cl and BrO concentrations during no-cloud phases. In addition, in the Hoffmann model Cl and BrO are taken up by the cloud droplets lowering their concentration during cloud phases, while in ADCHAM this has not been incorporated yet. However,

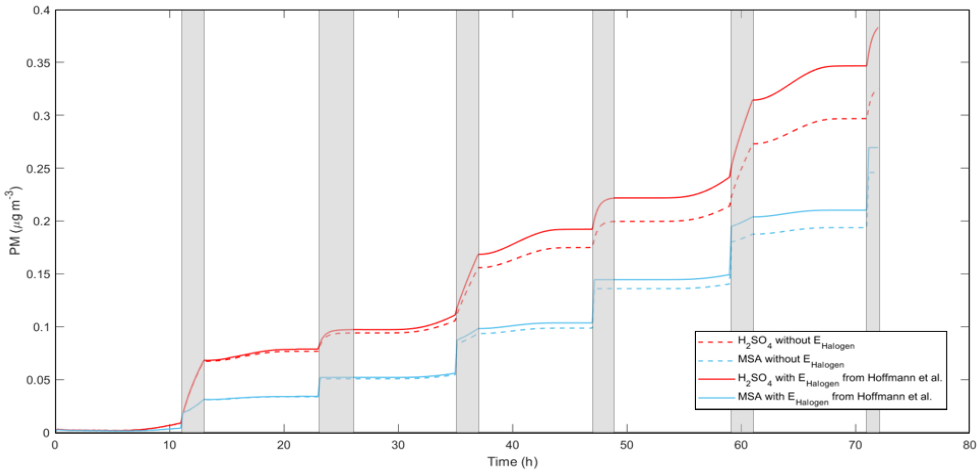

Figure 12: The ADCHAM simulations of the total aerosol particle mass from MSA and H_2SO_4 for with and without Halogens emission. The grey shaded areas display the cloud passages.

both figure 12 and 13 show the a definite, non-negligible effect of halogens on the DMS oxidation and the oxidation products.

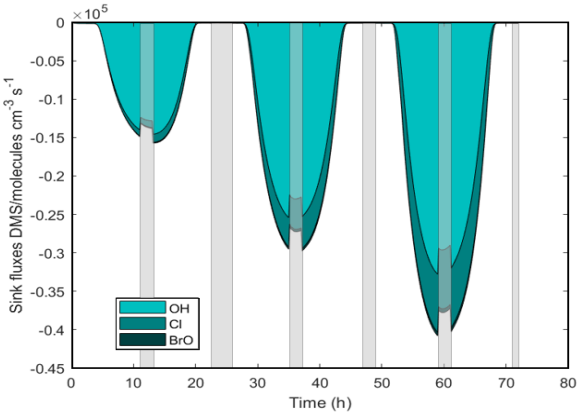

Figure 13: The simulated sink fluxes of DMS to bromine oxide (BrO), chlorine (Cl) and hydroxyl radicals (OH) shown in an stacked area graph.

Moreover, the figure 12 shows a general increase of particle mass during aqueous cloud phases, implying that DMS aqueous-phase reactions also strongly affect the DMS oxidation products. Further, an increased mass but not an increased particle number in the aerosol may decrease the impact of DMS aerosols on indirect radiative forcing and implying that neglecting aqueous-phase and halogen reactions could lead to an overestimation of the indirect radiative effect of DMS aerosols.

All in all, the ADCHAM simulation without halogen chemistry shows a good agreement with the analogous results from Hoffmann et al. [3]. The new particle formation is most likely more influenced by the magnitude of the ammonia emissions over the ocean than the DMS emissions, but higher DMS emission show an increase in the PN simulations.

The aqueous-phase reactions show a definite increase in the aerosol mass during the cloud phases. Both, halogen and aqueous-phase reactions of DMS show a strong impact on the product yield of MSA and H_2SO_4, increasing the need for current climate models to include both processes to increase their accuracy.

5 Outlook

In conclusion, this thesis confirmed and gave insight into the importance of the DMS multi-phase, DMS-halogen reactions, and the uncertainties in the DMS oxidation and oxidation products leading to the secondary aerosol formation. The butanol-OH experiments highlighted the difficulties of the smog-chamber experiments, showing that the parametrisation of the UV-light intensity should be further investigated for humid experiments. For future laboratory simulations, the ammonia concentration in the chamber should be measured, since it poses a large unknown in the simulation and is essential for the particle formation. Further, there are still many unknowns in the multi-phase and halogen reactions of DMS and its oxidation products. In future work, the dissolution of HPMTF in clouds could be investigated as well as finding an optimal representation of the halogen chemistry. The ADCHAM model was set-up to run some of the halogen chemistry representation of Bräuer et al. [5] which includes more than 200 halogen reactions pathways. This should be looked into in the future to get a better representation of the bromine and chlorine species in the cloud and aerosol particle aqueous-phases. The total climate impact of DMS aerosols is still uncertain and will be until an accurate representation of the DMS-oxidation scheme and it oxidation product is established.

Acknowledgments

I would like to thank my supervisor Pontus Roldin for carefully guiding me through aerosol modelling and always finding the time to give me advice. I truly learned a lot and I am grateful I had the opportunity to look over his shoulder, but most importantly, I am thankful for being able to try and discuss ideas that shaped this thesis work and my understanding.

References

[1] Jacob D. Introduction to Atmospheric Chemistry. 1st ed. Princeton: Princeton University Press; 1999.

[2] Charlson R, Lovelock J, Andreae M, et al. Oceanic phytoplankton, atmospheric sulphur, cloud albedo and climate. Nature. 1987;326:655–661. Available from: https://doi.org/10.1038/326655a0.

[3] Hoffmann E, Tilgner A, Schrödner R, Bräuer P, Wolke R, Herrmann H. An advanced modeling study on the impacts and atmospheric implications of multiphase dimethyl sulfide chemistry. Proceedings of the National Academy of Sciences. 2016;133(42):11776–11781. Available from: https://www.pnas.org/content/113/42/11776.

[4] Barnes I, Hjorth J, Mihalopoulos N. Dimethyl Sulfide and Dimethyl Sulfoxide and Their Oxidation in the Atmosphere. Chemical reviews. 2006 04;106:940–75. Available from: https://doi.org/10.1021/cr020529.

[5] Bräuer P, Tilgner A, Wolke R, Herrmann H. Mechanism development and modelling of tropospheric multiphase halogen chemistry: The CAPRAM Halogen Module 2.0 (HM2). JOURNAL OF ATMOSPHERIC CHEMISTRY. 2013 03;70:19–52.

[6] Roldin P, Eriksson AC, Nordin EZ, Hermansson E, Mogensen D, Rusanen A, et al. Modelling non-equilibrium secondary organic aerosol formation and evaporation with the aerosol dynamics, gas- and particle-phase chemistry kinetic multilayer model ADCHAM. Atmospheric Chemistry and Physics. 2014;14(15):7953–7993. Available from: https://doi.org/10.5194/acp-14-7953-2014.

[7] Veres PR, Neuman JA, Bertram TH, Assaf E, Wolfe GM, Williamson CJ, et al. Global airborne sampling reveals a previously unobserved dimethyl sulfide oxidation mechanism in the marine atmosphere. Proceedings of the National Academy of Sciences. 2020;117(9):4505–4510. Available from: https://www.pnas.org/content/117/9/4505.

[8] Hinds W. Aerosol Technology: Properties, Behavior, and Measurement of Airborne Particles. 2nd ed. New York: John Wiley Sons; 1999.

[9] Glasius M, Goldstein AH. Recent Discoveries and Future Challenges in Atmospheric Organic Chemistry. Environmental Science & Technology. 2016;50(6):2754–2764. Available from: https://doi.org/10.1021/acs.est.5b05105.

[10] Ivlev LS. 12. In: Atmospheric Aerosols. John Wiley Sons, Ltd; 2010. p. 343–378. Available from: https://onlinelibrary.wiley.com/doi/abs/10.1002/9783527630134.ch12.

[11] Boucher O, Randall D, et al. 2013: Clouds and Aerosols. In: Climate Change 2013: The Physical Science Basis. Contribution of Working Group I to the Fifth Assessment

Report of the Intergovernmental Panel on Climate Change [T.F. Stocker et al.]. Cambridge University Press, Cambridge, United Kingdom and New York, NY, USA; 2013. p. 571–658. Available from: https://www.ipcc.ch/report/ar5/wg1/.

[12] Stocker TF, Qin D, Plattner GK, Alexander LV, Allen SK, Bindoff NL, et al. 2013: Technical Summary. In: Climate Change. In: Climate Change 2013: The Physical Science Basis. Contribution of Working Group I to the Fifth Assessment Report of the Intergovernmental Panel on Climate Change [T.F. Stocker et al.]. Cambridge University Press, Cambridge, United Kingdom and New York, NY, USA; 2013. p. 571–658. Available from: https://www.ipcc.ch/report/ar5/wg1/.

[13] Albu M, Barnes I, Becker KH, Patroescu-Klotz I, Benter T, Mocanu R. Ft-Ir Product Study On The Oh Radical Initiated Oxidation Of Dimethyl Sulfide: Temperature And O2 Partial Pressure Dependence. In: Barnes I, Kharytonov MM, editors. Simulation and Assessment of Chemical Processes in a Multiphase Environment. Dordrecht: Springer Netherlands; 2008. p. 501–513.

[14] Berndt T, Scholz W, Mentler B, Fischer L, Hoffmann EH, Tilgner A, et al. Fast Peroxy Radical Isomerization and OH Recycling in the Reaction of OH Radicals with Dimethyl Sulfide. The Journal of Physical Chemistry Letters. 2019;10(21):6478–6483. PMID: 31589452. Available from: https://doi.org/10.1021/acs.jpclett.9b02567.

[15] Wu R, Wang S, Wang L. New Mechanism for the Atmospheric Oxidation of Dimethyl Sulfide. The Importance of Intramolecular Hydrogen Shift in a CH3SCH2OO Radical. The Journal of Physical Chemistry A. 2015;119(1):112–117. PMID: 25486505. Available from: https://doi.org/10.1021/jp511616j.

[16] Kristensen K, Jensen LN, Glasius M, Bilde, M. The effect of sub-zero temperature on the formation and composition of secondary organic aerosol from ozonolysis of alpha-pinene. Environ Sci: Processes Impacts. 2017;19(10):1220–1234. Available from: http://dx.doi.org/10.1039/C7EM00231A.

[17] Olenius T, Kupiainen-Määttä O, Ortega IK, Kurtén T, Vehkamäki H. Free energy barrier in the growth of sulfuric acid-ammonia and sulfuric acid-dimethylamine clusters. . 2013 Aug;139(8):084312–084312.

[18] Zádor J, Turányi T, Wirtz KW, Pilling MJ. Measurement and investigation of chamber radical sources in the European Photoreactor (EUPHORE). Journal of Atmospheric Chemistry. 2006;55:147–166.